

RNA interference targeting survivin exerts antitumoral effects in vitro and in established glioma xenografts in vivo

Sandy Hendruschk, Ralf Wiedemuth, Achim Aigner, Katrin Töpfer, Marc Cartellieri, Daniel Martin, Matthias Kirsch, Chrysanthy Ikonomidou, Gabriele Schackert, and Achim Temme

Department of Neurosurgery (S.H., R.W., K.T., D.M., M.K., G.S., A.T.), University Hospital Carl Gustav Carus and Institute of Immunology (M.C.), Medical Faculty Carl Gustav Carus, Technical University Dresden, Dresden; Institute of Pharmacology, Philipps University, Faculty of Medicine, Marburg, Germany (A.A.); Department of Pediatric Neurology, University of Wisconsin-Madison, WI, USA (C.I.)

Malignant glioma represents the most common primary adult brain tumor in Western industrialized countries. Despite aggressive treatment modalities, the median survival duration for patients with glioblastoma multiforme (GBM), the highest grade malignant glioma, has not improved significantly over past decades. One promising approach to deal with GBM is the inactivation of proteins essential for survival or progression of glioma cells by means of RNA interference (RNAi) techniques. A likely candidate for an RNAi therapy of gliomas is the inhibitor of apoptosis protein survivin. Survivin is involved in 2 main cellular processes—cell division and inhibition of apoptosis. We show here that stable RNAi of survivin induced polyploidy, apoptosis, and impaired proliferation of human U343-MG, U373-MG, H4, and U87-MG cells and of primary glioblastoma cells. Proteome profiler arrays using U373-MG cells identified a novel set of differentially expressed genes upon RNAi-mediated survivin knockdown. In particular, the death receptor TRAIL R2/DR5 was strongly upregulated in survivin-depleted glioma cells, inducing an enhanced cytotoxic response of allogeneic human NK cells. Moreover, an experimental in vivo therapy using polyethylenimine (PEI)/siRNA complexes for survivin knockdown efficiently blocked tumor growth of established

subcutaneous U373-MG tumors and enhanced survival of NMRI^{nu/nu} mice orthotopically transplanted with U87-MG cells. We conclude that survivin is functionally relevant in gliomas and that PEI-mediated exogenous delivery of siRNA targeting survivin is a promising strategy for glioblastoma therapy.

Keywords: glioblastoma, RNAi, survivin.

In Western industrialized countries, malignant glioma represents the most common primary adult brain tumor.^{1,2} Despite aggressive treatment with surgical resection followed by radiotherapy and chemotherapy, these tumors ultimately recur.^{3–5} The median duration of survival for patients with the highest grade malignant glioma, glioblastoma multiforme (GBM), has not improved significantly over the past decades, remaining at 12–15 months.⁵ The infiltrative nature of the tumor, the impracticability of optimal resection, and the resistance to combined chemo- and radiation therapy lead to a 5-year survival rate of <2%.³ This extraordinarily high morbidity has triggered a vigorous search for novel and more specific therapeutic approaches.

One promising avenue to deal with glioma—in particular, with glioblastoma—is the inactivation of proteins that are essential for survival or progression by RNA interference (RNAi), finally leading to the destruction of the tumor cells. Major targets for RNAi therapy include oncogenes and genes that are involved in angiogenesis, metastasis, survival, anti-apoptosis, and resistance to chemotherapy (for review, see Ashihara et al⁶), yet they must be carefully selected. Optimal RNAi

Received June 22, 2010; accepted June 1, 2011.

Corresponding Author: Achim Temme, Professor, Department of Neurosurgery, Section Experimental Neurosurgery/Tumor Immunology, University Hospital Carl Gustav Carus, Technical University Dresden, Fetscherstrasse 74, 01307 Dresden, Germany (achim.temme@uniklinikum-dresden.de).

targets to treat tumors include molecules that are functionally relevant in the tumor and, to avoid site effects, should not be expressed at significant levels in normal tissues. In addition, when using a 1-target-approach, RNAi-targets should be chosen that cannot be functionally compensated by other members of the same protein family.

Among the family of inhibitor of apoptosis proteins (IAPs), survivin has received special attention because it is highly expressed in cancer tissues and cancer cell lines.⁷ A large comparative scale analysis of human transcripts in tumor and normal tissue identified survivin as 1 of the 4 most highly expressed genes selectively found in tumors.⁸ Survivin is also expressed in human gliomas,⁹ where increased levels of expression have been described to correlate with higher malignancy of the tumor and, therefore, with a poorer prognosis.^{10–12} Survivin exerts an anti-apoptotic function through its baculoviral IAP repeats domain by binding to activated caspases.^{13,14} Furthermore, an anti-apoptotic capacity of survivin through inhibition of the second mitochondria derived apoptosis inducing factor Smac/DIABLO¹⁵ and of the apoptosis inducing factor has been reported.¹⁶ The gene for survivin, *birc5*, is located in 17q25 and gives rise to a dominant expressed isoform with a molecular weight of 16.5 kD.⁷ Survivin is periodically expressed during the cell cycle, with peak expression in the G₂ and the M phase.¹⁷ Interestingly, its expression is impaired by p53, and loss of p53 function, which is often observed in cancer, increases *birc5* transcription.^{18,19} It is anticipated that an increase in survivin steady-state levels enhances the resistance of cancer cells to chemotherapeutic drugs or radiation.²⁰ Thus far, these properties of survivin are not unique, and RNAi-mediated knockdown of survivin might be compensated by the upregulation of other IAP family members, such as XIAP or cIAP, or by increased expression of anti-apoptotic members of the bcl2-family, such as bcl2 and bcl-XL. However, to date, it is widely accepted that survivin plays an additional and unique role in the regulation of mitotic events.^{21–24} The mitotic localization of survivin is consistent with the proteins described as chromosomal passenger proteins.^{23–25} During early mitosis, survivin associates around chromosomes together with its protein partners Aurora B, borealin, and inner centromeric protein—in particular, at the kinetochores in metaphase.²⁵ Cells with impaired function of survivin or of one of its partners due to RNAi-mediated inhibition or expression of dominant-negative mutants showed comparable phenotypes (ie, disturbed segregation of chromosomes and defective cytokinesis).^{24–27} Furthermore, the disruption of the genetic locus of survivin was not compensated and led to an embryonically lethal phenotype in homozygous mice.²³

We hypothesized that the selective inhibition of glioma cells by RNAi-mediated knockdown of survivin may represent a reasonable therapeutic strategy for the treatment of malignant brain tumors. Therefore, we employed retroviral shRNA expression vectors and the nonviral delivery of siRNAs to silence survivin in glioma cells and glioma xenografts, respectively, and analyzed the effects. We found that survivin knockdown

led to mitotic defects and decreased cell proliferation. In particular, an impaired long-term clonogenic survival was noted in H4 and U373-MG as well as in primary glioblastoma cells after knockdown of survivin. In addition, a strong increase in death receptor TRAIL R2/DR5 expression was detected, which rendered glioma cells more susceptible to allogeneic human NK cells. The treatment of immune-deficient mice bearing subcutaneous U373-MG or orthotopic U87-MG tumors, with polyethylenimine (PEI)-complexed siRNA against survivin resulted in a significant decrease of tumor growth and increased survival time, respectively, indicating the potential of RNAi approaches for survivin inhibition as a feasible therapeutic option in GBM.

Materials and Methods

Cell Culture, Determination of Proliferation, and Clonogenic Survival

U373-MG is a glioblastoma/astrocytoma-derived cell line; U343-MG, U87-MG, and H4 are glioblastoma-derived cell lines. The cell lines were kindly provided by H. K. Schackert (Medical Faculty, Technical University-Dresden, Dresden, Germany). The primary glioblastoma cell lines DD-T3, DD-T4, and DD-HT7606 were obtained in the course of surgery of glioblastoma patients with informed consent and approval of the local ethics committee. Primary glioblastoma cells of passages 8–10 and human glioma cell lines were maintained on poly-L-lysine coated plasticware and in Basal Minimal Eagle medium (Invitrogen) supplemented with 2 mM L-glutamine and 1% nonessential amino acids (Biochrom). Two hundred ninety-three T cells were human embryonic kidney cells. They were cultured in Dulbecco's modified Eagle medium containing 4.5 g/L glucose (PAA Laboratories). The medium was supplemented with 10% heat-inactivated fetal calf serum, 100 U/mL penicillin, and 100 µg/mL streptomycin (both from Invitrogen). Primary human NK cells were isolated using a negative depletion kit (Miltenyi Biotec) and stimulated with NKp46/CD2 beads (Miltenyi Biotec) and 500 IU rhIL-2 (Immunotools). After 5 days, the NK cells were used for the experiments. All experiments with human NK cells were approved by the local ethical committee of the Medical Faculty Carl Gustav Carus (Technical University-Dresden). Expression of TRAIL and CD95 ligand was tested by FACS analysis using specific antibodies against TRAIL and CD95L (both BD Biosciences) and Cy3- or FITC-coupled secondary antibodies (Dianova). Cell proliferation of human glioma cells was assessed by Trypan blue staining and counting of viable cells using a hemacytometer. Cells (1×10^5) were plated in triplicates on 30-mm dishes and 24 h later cells were transduced with retroviral vectors. Twenty-four h, 72 h, and 5 days after transduction, cell numbers were determined. Long-term survival of transduced glioma cells was tested by plating quadruplicates of 1000 cells/dish for every vector transduction onto 10-cm dishes. After

3 weeks U373-MG and H4 cells and after 5 weeks primary GBM cells were stained with Giemsa, and the number of clones was quantified. At least 2 independent experiments were performed for each cell line. The Student *t* test was used for statistical analysis.

shRNA-Retroviral Vectors and Transduction

For the transduction of DNA-sequences encoding shRNA-molecules, the self-inactivating retroviral Moloney murine leukemia virus backbone pRVH-1 was used. This vector contains a H1 polymerase III promoter for the expression of shRNA molecules in reverse orientation. pRVH1 was digested with EcoRI and NotI and ligated with a cytomegalovirus immediate early promoter and enhanced green fluorescent protein (EGFP) reporter gene fragment containing appropriate restriction sites, resulting in the vector pRVH-N1-EGFP. For some experiments, a RVH1-puro vector was used. On the basis of 2 previously described survivin target sequences, DNA oligonucleotides with appropriate restriction site overhangs shown in *italic* (shSurvivin #237 upper strand: 5'-*gatccccgaggctggcttcacactttcaagagaagtgatgaagccagcctcttttggc-3'*; shSurvivin #237 bottom strand: 5'-*tcgagccaaaaagaggctgcttcacacttcttgaagtggatgaagccagcctcggg-3'*;²⁸ shSurvivin #433 upper strand: 5'-*gatccccgaattaacccttggtgaattcaagagaattcaccaagggttaattcttttggc-3'*, shSurvivin #433 bottom strand: 5'-*tcgagccaaaaagaattaacccttggtgaattcttgaattcaccaagggttaattcggg-3'*²⁹) were synthesized (Eurofins MWG Biotech), and after annealing of the single strands, the shRNA-encoding fragment was ligated into the BglII/Sall-restriction sites of pRVH-N1-EGFP and pRVH-puro, respectively. As negative control, we included a previously described shRNA against luciferase.³⁰

Retroviral particles were generated as described previously.³¹ In brief, 293 T cells were cotransfected with an expression construct for gag-pol (pHIT60), the MoMuLV-based retroviral vectors and the vesicular stomatitis virus G-protein (pMD.G2). Viral supernatants were harvested 48 and 72 h after transfection. Target cells (10^5) cells were plated in 30-mm dishes 1 day before transduction and were transduced with retroviral supernatants. Transduction efficacies were usually in the range of 90%–98%, as determined by FACS-analysis of EGFP-positive cells. Glioma cells, which were transduced with pRVH1-puro vectors, were additionally selected using 10 µg/mL puromycin (Invitrogen) for 24 h.

Indirect Immunofluorescence Analysis

Cells grown on poly-L-lysine-mounted glass slides and 6-µm slices from frozen brain tissues were fixated for 20 min with 4% paraformaldehyde in phosphate-buffered saline (PBS). Samples were treated with ice-cold permeabilization solution (0.1% sodium citrate in PBS, 0.1% Triton X-100) for 5 min. Samples were incubated for 1 h with a polyclonal rabbit anti-survivin antibody (R&D Systems; dilution, 1:200) or were analyzed using a monoclonal anti rabbit Ki67 (Epitomics).

Samples were washed 3 times with PBS + 0.1% BSA and were subsequently incubated with a secondary anti-rabbit immunoglobulin (Ig) G, Cy3 conjugated antibody (dilution, 1:200; Jackson IR) for 1 h. DNA counterstaining was accomplished with Hoechst33342 solution (10 µg/mL) for 5 min. Finally, the stained cells and tissues were washed 3 times in PBS/0.1% BSA and once in double-distilled water, prior to examination by confocal laser scanning microscopy (Leica SP5 inverse MP) or standard immunofluorescence microscopy (Olympus IX70). The Ki67-proliferation index was calculated by analyzing the average percentage of fluorescence-labeled cells in ≥ 14 random fields from different sections at $\times 400$ magnification. Statistical analysis was performed using the Student *t* test.

Proteome Profiler Array and Western Blot Analysis

For immunoblot analysis, 10^5 cells grown in 6-well plates were harvested in 75 µL $2\times$ Laemmli protein sample buffer (Sigma). Samples were subsequently boiled for 10 min and placed in an ultrasonic bath for 10 min. Equal protein amounts of lysate fractions were loaded onto polyacrylamide gels and, after separation, blotted onto PVDF membranes. Subsequently, membranes were washed 3 times for 10 min in TBS + 2% Triton X-100, 0.5% Tween 20 (TBS-TT) and another 10 min in TBS. The membranes were probed with rabbit polyclonal anti-survivin (R&D Systems), and signals were developed as described below. For loading control, blots were stripped and probed with a monoclonal anti-tubulin antibody (Sigma) or a monoclonal anti GAPDH (dilution, 1:1000; Cell signaling). Cell-cycle arrest was investigated using an anti-p21^{wat/cip} antibody (monoclonal rabbit; dilution, 1:1000; Cell Signaling Technology), and induction of apoptosis was analyzed by an anti-caspase 3 antibody (mouse monoclonal; dilution, 1:1000; Cell Signaling). After incubation with the primary antibodies, the membranes were washed 3 times with TBS-TT and 1×10 min with TBS buffer. Subsequently, the membranes were incubated for 1 h with appropriate secondary antibodies conjugated with HRP (dilution, 1:1000; Dako). The membranes were washed again, signals were developed with ECLplus detection solution (GE Healthcare), and chemoluminescence was detected in a LAS3000 device. The effects of survivin-RNAi on U373-MG cells were assessed by the apoptosis proteome profiler kit (R&D Systems) in accordance with the instructions of the provider. The kit allows the simultaneous analysis of the cell cycle, stress response, and expression of apoptosis inhibiting proteins and of pro- and anti-apoptotic members of the bcl-2- protein family and proteins involved in cell cycle arrest. In brief, 6×10^6 U373-MG cells were seeded in T75 culture flasks and transduced with 12 mL viral supernatants representing an multiplicity of infection of 20. Three days after transduction, the cells were harvested, the protein concentration was determined, and knockdown of survivin was confirmed by immunoblotting. Subsequently, 250 µL of lysate representing 150 µg of total protein was diluted in 1.25 mL of Array buffer 1. Arrays were

pre-incubated in 1.5 mL of Array buffer 1 prior to incubating the arrays in the diluted lysate at 4°C overnight. The arrays were washed 3 times using wash buffer, incubated for 4 h with the detection antibody cocktail (dilution, 1:100 in 1 × array buffer 1), and after repeated washing arrays, incubated with a Streptavidin-HRP-solution (dilution, 1:2000). Signals were detected using the ECLplus reagent (GE Healthcare) and the LAS3000 device. Images were taken for several time intervals and analyzed using imageJ software (National Institutes of Health) and by subtracting PBS background levels (negative control) from sample signal levels. Experiments were performed at least twice. Statistical analysis was performed using the Student *t* test.

Flow Cytometry for Cell Cycle Analysis, BrdU Incorporation and TRAIL R2/D5 Expression

Analysis of the cell cycle and apoptosis was determined by flow cytometry (FACScan; BD Biosciences) of propidium iodide-stained cells using Cell Quest Software (BD Biosciences). In brief, nonsynchronized cells were washed in PBS and fixed in 70% (v/v) ethanol. After centrifugation of the cells at 600 g for 10 min at 20°C, the cell pellet was suspended in 0.5 mL of DNA-extraction buffer (4 mM citric acid in 0.2 M Na₂HPO₄; pH, 7.8). After 5 min incubation at room temperature, the cells were spun down at 600 g. The cells were washed once with PBS, followed by incubation in PBS containing 40 µg/mL propidium iodide (Sigma) and 200 µg/mL RNase A (Sigma) for 1 h at room temperature in the dark. Stained nuclei were analyzed using a Becton Dickinson FACScan (BD Biosciences) with at least 10,000 events/determination. Cells that displayed propidium iodide-fluorescence emissions lower than the 2N-DNA peak were considered to be apoptotic (hypodiploid) cells. FACS analysis of TRAIL R2/DR5, Fas-L, and TRAIL expression was accomplished using monoclonal mouse anti TRAIL R2/D5 (Acris) and monoclonal mouse anti Fas-L and TRAIL antibodies (both from BD Biosciences) and secondary goat anti-mouse IgG coupled to FITC. Appropriate isotype controls were included as controls. For DNA-synthesis analysis, cells were incubated with 10 µM of BrdU (Sigma) for 45 min. Then, cells were harvested and spun down at 330 g for 8 min. The cell pellets were fixed in cold (-20°C) 70% (v/v) ethanol at 4°C. DNA of 2 × 10⁵ cells/sample were denatured by incubation with 2 N HCl-0.5% Triton X-100 for 30 min at room temperature, followed by neutralization with 0.1 M Na₂B₄O₇ × 10H₂O (pH8.5) for 30 min at room temperature. Subsequently, cells were stained with fluorescein isothiocyanate-conjugated anti-BrdU antibody (BD; dilution, 1:12.5) in PBS containing 1% BSA and 0.3% Triton-X-100 for 45 min at room temperature in the dark. DNA was counterstained using propidium iodide as described above, and gated viable cells were measured by flow cytometry. An appropriate FITC-conjugated isotype control was included in the

analysis. Experiments were performed in triplicates and were performed at least twice. Statistical analysis was performed with the Student *t* test.

⁵¹Cr Release Assay

The ability of primary human NK cells to recognize and kill U373-MG and H4 glioma cells upon knockdown of survivin expression was analyzed in a ⁵¹Cr release assay. In brief, 5 days after transduction (1 × 10⁶), shLuc- or shSurvivin #433-transduced glioma target cells were labeled with 100 µCi of ⁵¹Cr (PerkinElmer Life Sciences) for 1 h at 37°C and then washed 4 times with PBS. Labeled target cells were plated as triplicates in round-bottom 96-well plates at 3 × 10³/well and were incubated with NK effector cells at different effector-target (E:T) ratios for 4 h and 8 h, respectively. Released ⁵¹Cr was determined in a beta counter (PerkinElmer Life Sciences). Maximal and minimal release was measured by treating labeled cells with 2% Triton X-100 or medium alone, respectively. The specific cytotoxicity was calculated according to the following formula: percent-specific lysis = 100 × [(cpm experimental release - cpm spontaneous release)/(cpm maximum release - cpm spontaneous release)].

Tumor Growth in Nude Mice and Experimental siRNA Therapy

Nine-week-old NMRI^{nu/nu} mice were obtained from the animal facility of the University of Dresden. Mice were held under standardized pathogen-free conditions with ad libitum access to food and water. Experiments were approved by the responsible local authorities according to the German animal protection law. For the experimental PEI/siRNA therapy of established subcutaneous tumors, U373-MG cells (1 × 10⁶ in 200 µL PBS) were injected into the right flank of the mice. After 3 weeks, the established wild-type tumors were measured using a digital caliper, and the mice were subdivided in 3 groups with the same mean tumor diameter. For the experiments, we used a siRNA (siSurvivin), which targets the same complementary mRNA sequence as the small hairpin RNA shSurvivin #433. Chemically unmodified siRNAs siSurvivin (sense: 5'-gaauaacccuuggu-gaa(tt)-3'; antisense: 5'-auucaccaaggguuuuuuuc(tt)-3') and siLuc control (sense: 5'-cguacgcggauacuucga(tt)-3'; antisense: 5'-ucgaaguauucgcggauucg(tt)-3') were synthesized, purified using HPLC (Eurofins MWG Biotech), and complexed with low-molecular weight PEI F25-LMW, as described elsewhere.³² Every 2 days, mice received intraperitoneal injections of 10 µg (400 µg/kg bodyweight) PEI-complexed siRNA against survivin or firefly luciferase (siLuc) in 150 µL of PBS, starting at day 1 of treatment, for a total of 10 injections. As additional negative control, a group of mice receiving intraperitoneal injections of 150 µL of PBS was included to exclude nonspecific effects of PEI on tumor growth. Tumor sizes were measured in both directions by a digital caliper every 2 days. After calculating the mean

of the tumor diameter, the volume of each tumor was calculated by the formula $V_{\text{Tumor}} = 1/6 \times \pi \times d^3$. Mice were killed at day 21 after the start of the PEI/siRNA treatment, and the tumors were prepared and used for mRNA-analysis and histology. The experiments were performed twice, with comparable results. In total, 10 controls, 11 siLuc-treated mice, and 11 siSurvivin-treated mice were analyzed. For the experimental PEI/siRNA treatment of intracranial gliomas, we stereotactically transplanted U87-MG cells in accordance with the guide screw method described by Brockmann et al.³³ Guide screws were implanted 3 days before injection of 1×10^6 U87-MG glioma cells in 10 μL of PBS into the right brain hemisphere of mice. Three days after transplantation of tumor cells, the experimental siRNA therapy was started with daily stereotactical injections of 2.5 μg of PEI-complexed siSurvivin and siLuc for 10 days. Mice were killed when neurological symptoms became apparent. The experiments were performed twice with comparable results. In total, survival of 13 siLuc-treated mice, and of 12 siSurvivin-treated mice was monitored. Additional mice, including 4 siLuc-treated mice bearing neurological symptoms and 3 siSurv-treated mice having no neurological deficits, were killed at day 17 and brain cryoslices were used for hematoxylin staining, Terminal deoxynucleotidyl transferase nick end labeling (TUNEL), and Ki67 analysis. Statistical analysis of tumor growth and survival were performed with the Student *t* test and by log-rank test, respectively.

mRNA Preparation, cDNA Synthesis, and Quantitative (Q) Real-Time Polymerase Chain Reaction (QPCR)

Total mRNA of tumor samples was prepared using a QiaShredder and the RNeasy kit from Qiagen in accordance with the instructions of the provider. cDNA was generated using 1 μg of total mRNA, Oligo (dT)₁₂₋₁₅ primer (GE Healthcare), and the Omniscript reverse-transcriptase kit (Qiagen). On the basis of the LightCycler (LC) technology (Roche), QPCR assays were performed to quantify the mRNA expression of survivin and of the housekeeping gene β -actin. The levels of a specific PCR product were determined by the use of TaqMan probes (β -actin-TM: 5'-6FAM-CAGCTTCA CCACCACggCCAXT-PH; Survivin-TM: 5'-6FAM-CCACTgCCCCACTgAgAACgAgCXT-PH). As PCR primers, we used LC-BETA_ACTIN_FOR 5'-tca ccgagcggct-3', LC_BETA_ACTIN_REV 5'-taatgt cacgcatttccc-3', LC_SURVIVIN_FOR 5'-gccgagctggc ttca-3', and LC_SURVIVIN-REV 5'-gaagaactgg gccaagtct-3'. The levels of all transcripts were determined by an amplification protocol consisting of a denaturation step at 95°C for 10 min, followed by 40 cycles with a 95°C denaturation step for 15 s, 61°C annealing for 5 s, and a 72°C extension step of 5 s. Standard curves were generated applying dilutions over 6 log scales (10^1 – 10^6) per capillary using a plasmid encoding human β -actin and a plasmid encoding human survivin and were used to calculate the amplification products. All measurements were performed with aliquots from the

same cDNA batches to guarantee standardized and comparable conditions. A negative control (no template) was included in each of the PCR runs. The cDNA copy numbers of *survivin* mRNAs were normalized to the quantitative measurements of β -actin mRNA levels. All PCR runs were repeated twice to ensure reproducibility and reliability and were analyzed by the LC quantification software, version 3.5 (Roche). For statistical analysis, the Student *t* test was used.

TUNEL Apoptosis Assay

Analysis of apoptosis in tumors was performed using TUNEL (in situ cell death detection kit; Roche) using the protocol recommended by the supplier. DNA counterstaining was accomplished with Hoechst33342 solution. Finally, cells were washed 3 times in PBS/0.1% BSA and once in double-distilled water prior to examination by standard immunofluorescence microscopy (Olympus IX70). The apoptosis index was calculated by analyzing the mean percentage of BrdU-FITC-labeled cells in ≥ 10 random fields from different sections at $\times 400$ magnification. Statistical analysis was performed using the Student *t* test.

Determination of Interferon (IFN)- α Serum Levels

For analysis of IFN- α levels in PEI/siRNA-treated animals (each group contained 4 animals), serum of C57BL/6-mice and of NMRI mice treated with PEI-complexed survivin siRNA or luciferase siRNA, respectively, was collected. As positive control, we included mice intraperitoneally injected with 150 μL (100 $\mu\text{g}/\text{mL}$) of polyinosinic-polycytidylic acid (in 0.9% NaCl in endotoxin-free H₂O; Cayla InvivoGen Europe), which is known to activate TLR3 and to increase IFN- α levels. The blood was allowed to clot for 2 h at room temperature and was centrifuged for 10 min at 400 \times g. The aqueous phase representing the serum was removed, diluted 1:1 and 1:2 with PBS, and analyzed in triplicates using an IFN- α enzyme-linked immunosorbent assay (Mu-IFN- α ; PBL Biomedical Laboratories) in accordance with the instructions of the manufacturer.

Results

Stable Knockdown of Survivin Expression in Glioma Cells Results in Mitotic Defects and Impairs Glioma Cell Growth In Vitro

Retroviral expression vectors encoding EGFP and shRNAs targeting human survivin mRNA, or firefly luciferase mRNA as negative control, were transduced in glioma cell lines H4, U373-MG, U343-MG, and U87-MG. Western blot analysis of total protein lysates confirmed survivin protein expression in all tested glioma cell lines treated with shLuciferase and an efficient knockdown of survivin protein steady-state levels when

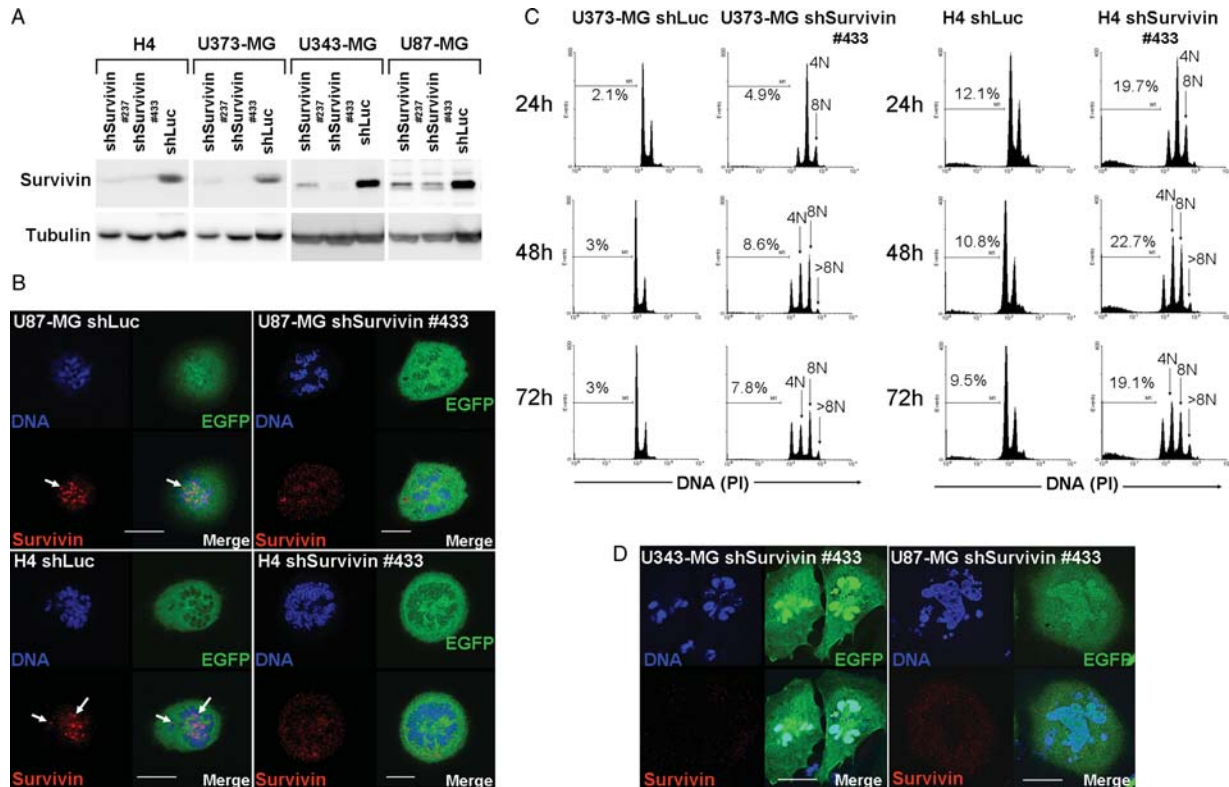


Fig. 1. Knockdown of survivin protein expression in glioma cell lines using small hairpin RNAs #237 and #433. (A) Glioma cell lines were transduced with retroviral pRVH-N1-EGFP vectors encoding the indicated shRNAs. Western blot analyses demonstrate efficient survivin knockdown compared to shLuc controls (shLuciferase-transduced cells). (B) Confocal laser scanning microscopy-based analysis of representative samples show the loss of survivin immunofluorescence at kinetochores of shSurvivin #433-transduced U86-MG and H4 glioma cells. In the images showing shLuciferase shRNA-treated cells, arrows indicate centromere regions of chromosomes that are positive for survivin. In contrast, note the increased number of chromosomes in the shSurvivin #433-treated cells. Bars represent 10 μ m. (C) Analysis of the DNA content in U373-MG glioma cells and H4 glioma cells, transduced with shSurvivin #433 or control (shLuciferase). Note the increase in cell numbers with a DNA content $>2N$ after knockdown of survivin. Arrows depict fractions of cells with DNA contents at 4N, 8N, and $>8N$. The percentage of cells containing DNA content less than the 2N peak (SubG1), representing apoptotic cells, is indicated as well. (D) Representative pictures showing the phenotype of shSurvivin #433-treated glioma cells. Note the increased cell size and the appearance of multiple nuclei in the survivin knockdown cells. Bars represent 25 μ m.

using the small-hairpin RNAs shSurvivin #237 and shSurvivin #433 (Fig. 1A). Indirect immunofluorescence analyses of all glioma cells with knockdown of survivin showed impaired or lost survivin immunosignals at the kinetochores of metaphase chromosomes, confirming a robust RNAi effect (representative images are depicted in Fig. 1B). Because no differences in the silencing effects of the shSurvivin #237 and #433 hairpins were observed, we used both throughout our experiments.

The inactivation of survivin caused polyploidy in all tested glioma cell lines, with the fastest effect after survivin knockdown being observed in H4 and U373-MG glioma cells. We therefore chose these glioma cell lines for additional experiments. When tested by FACS analysis of the cellular DNA content, the H4 and U373-MG cells developed remarkable amounts of cells with DNA content greater than 4N within 24 h (Fig. 1C). The fraction of cells with polyploidy genomes gradually increased over time. Notably, a time-dependent slight but significant increase in the fraction of apoptotic cells bearing hypodiploid genomes was detected in

U373-MG cells treated with shSurvivin (mean \pm standard deviation [SD], 10.1% \pm 2.4% at 72 h after transduction) compared with shLuc-transduced controls (mean \pm SD, 4.9 \pm 3.2% 72 h after transduction) (Fig. 1C). In contrast, the H4 cells showed a significantly larger fraction of apoptotic cells (mean \pm SD, 22.3% \pm 4.8%) when compared to the shLuc-transduced controls (mean \pm SD, 9.9% \pm 2.1%) already at 24 h after the shSurvivin transduction, but the apoptotic rate remained stable for all analyzed time points thereafter (Fig. 1C). Confocal laser-scanning microscopy using a specific antibody for survivin confirmed that the knockdown of survivin was associated with an increase in cell size and appearance of multiple nuclei in interphase (Fig. 1D). We hypothesized that knockdown of survivin in H4 and U373-MG cells led to an endoreplication without affecting cell cycle (ie, cell-cycle arrest). In line with this notion, Western blot analysis of p21^{waf/cip} induction, which hallmarks cell-cycle arrest, was not detected in U373 cells after knockdown of survivin (Fig. 2A). However, we observed a weak induction of

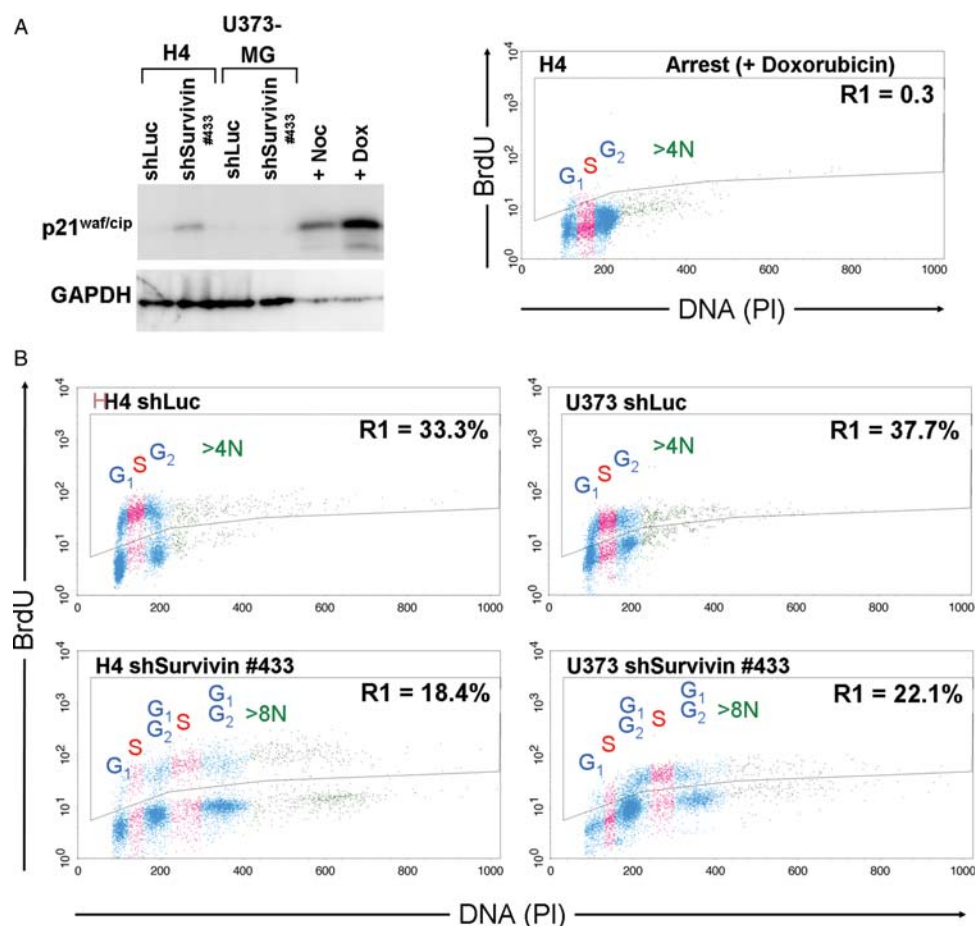


Fig. 2. Analysis of p21^{waf/cip} and BrdU incorporation in H4 and U373-MG cell with knockdown of survivin. (A) Western blot analysis of p21^{waf/cip} induction in H4 and U373-MG cells. Cells were transduced with shSurvivin #433 and shLuc. Seventy-two h after transduction, total cell lysates were prepared and subjected to electrophoresis. After blotting, p21^{waf/cip} expression was investigated. To demonstrate equal loading, the blot was stripped and probed with an antibody against the housekeeping protein GAPDH. As positive controls for p21^{waf/cip}, total protein lysates from HCT116 cells treated with nocodazole (+Noc) and doxorubicine (+Dox) were included. Note the weak p21^{waf/cip} signal in H4 cells with knockdown of survivin. That the H4 cells were able to arrest the cell cycle was demonstrated by using doxorubicin and subsequent BrdU incorporation analysis. (B) BrdU incorporation analysis of H4 and U373 cells 72 h after transduction of shSurvivin #433 and transduction with shLuc control, respectively, demonstrating that the cells did not arrest the cell cycle at 4N, 8N, and higher. Note that cells displaying polyploidy still incorporate BrdU.

p21^{waf/cip} in shSurvivin #433-treated H4 glioma cells. To analyze whether this weak p21^{waf/cip} expression was able to induce a cell-cycle arrest and to further investigate whether H4 and U373 bearing genomes >4N still were able to enter S-phase BrdU incorporation assays were performed. That H4 cells were able to arrest in the cell cycle was confirmed by incubating the cells with doxorubicin and subsequent BrdU incorporation analysis (Fig 2A). After analyzing the BrdU incorporation in cells with knockdown of survivin, it became clear that the knockdown of survivin led to a 40%–45% reduction in the fraction of BrdU-positive cells. However, H4 and U373-MG glioma cells with DNA contents at 4N, 8N, and higher especially did not arrest in the cell cycle and were still able to enter S-phase (Fig. 2B). Additional experiments demonstrated a statistically significant near abolishment of cell proliferation in U373-MG cells and H4 compared with the shLuc-transduced controls (Fig. 3A and B). In

particular, survivin knockdown significantly impaired long-term survival of U373-MG and H4 cells in a clonogenic assay (Fig. 3C and D).

Additional experiments with primary glioblastoma cell lines DD-T3, DD-T4, and DD-HT7606 revealed a similar phenotype after survivin knockdown, as observed in permanent glioma cell lines. An induction p21^{waf/cip} was not detected by Western blot analysis, neither in untreated controls nor in shLuc- and shSurvivin-transduced cells (Fig. 4A). However, knockdown of survivin resulted in an increase in cells having genomes >4N (Fig. 4B). The fraction of cells bearing genomes <2N (apoptotic cells) in the primary cell lines with knockdown of survivin were not increased in the DD-T3 and DD-T4 primary GBM cells compared with shLuc controls. In contrast, we noted significantly increased apoptosis rates in DD-HT7606 cells upon survivin RNAi (mean \pm SD, 33.8% \pm 3.2% 72 h after transduction) compared with those of shLuc-

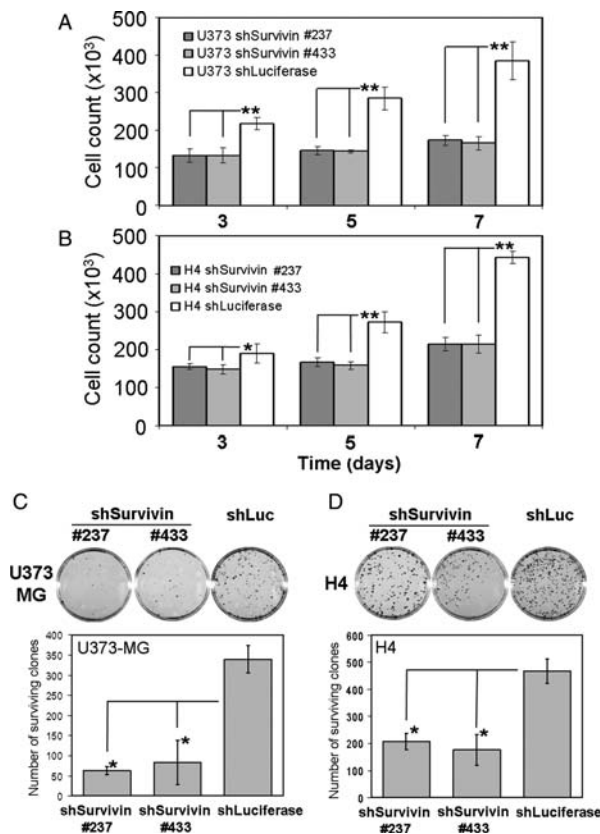


Fig. 3. Reduced proliferation and colony formation capacities of U373-MG and H4 glioma cells upon knockdown of survivin. (A and B) Proliferation of glioma cells after transduction of retroviral vectors encoding the depicted shRNA was determined by counting cell numbers. U373-MG (A) and H4 (B) cells transduced with shLuciferase exhibited a time-dependent increase in cell numbers. The numbers of U373-MG and H4 glioma cells transduced with shSurvivin #237 and shSurvivin #433 vectors were significantly lower, indicating the almost absence of proliferation ($*P < .05$; $**P < .01$). (C and D) Colony formation of U373-MG (C) and H4 (D) glioma cells transduced as indicated in the figure was assessed by plating of 10^3 cells per 10 cm dish in quadruplicates. After 3 weeks cells were stained with Giemsa and the mean \pm SEM number of clones was quantified. Data represent two independent transductions ($*P < .05$).

transduced controls (mean \pm SD, 23.1% \pm 2.4% 72 h after transduction) (Fig. 4B). Notably, we observed that the effect of survivin knockdown on clonogenic survival of primary glioblastoma cells was even stronger than measured for H4 and U373-MG cells. Here, clonogenic survival of primary glioma cells was nearly completely abolished after RNAi of survivin (Fig. 4C).

RNAi-Mediated Survivin Knockdown in U373-MG Cells Induced Expression of Hypoxia Inducible Factor-1 α (HIF-1 α) and of Death Receptor TRAIL R2

In addition to its function in the spindle checkpoint and cytokinesis, survivin functions as an inhibitor of apoptosis by blocking activated caspases and other pro-apoptotic molecules, such as Smac/DIABLO. To

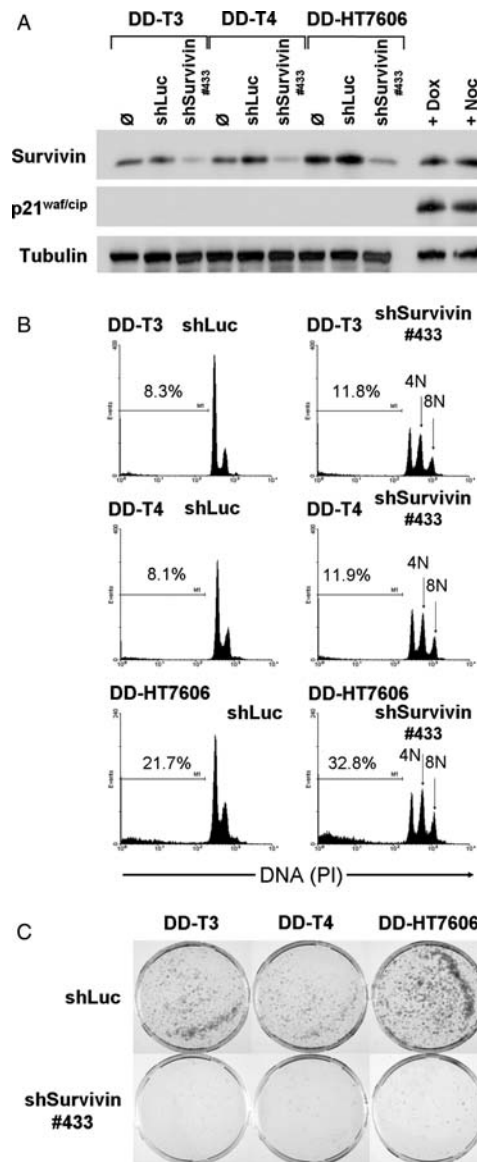


Fig. 4. Effects of survivin knockdown on primary glioblastoma multiforme (GBM) cells. (A) Total cell lysates from hSurvivin #433, shLuc-transduced and untreated primary GBM cells were subjected to Western blot analysis for confirming survivin knockdown and for investigating p21^{waf/cip} expression. As positive controls for p21^{waf/cip}, total protein lysates from HCT116 cells treated with nocodazole (+Noc) and doxorubicine (+Dox) were included. Equal loading was demonstrated using a tubulin antibody. (B) Analysis of the DNA content in primary glioblastoma cell lines DD-T3, DD-T4, and DD-HT7606 either transduced with shSurvivin #433 or control (shLuciferase). Note the increase in cell numbers with a DNA content $>2N$ upon survivin knockdown. Arrows depict fractions of cells with DNA contents at 4N and 8N. The percentage of cells containing DNA content less than the 2N peak (SubG1), representing apoptotic cells, is indicated as well. (C) Representative images of colony formation assays of primary GBM cells. Cells (10^3) were plated per 10-cm dish and, after 5 weeks, were stained with Giemsa. Note the nearly completely abolished clonogenic survival of shSurvivin #433 transduced primary GBM cells.

elucidate the effects of the survivin knockdown on apoptotic pathways, a proteome profiler analysis of U373-MG cells was performed (for details of analyzed proteins, see the Materials and methods section above). Significant alterations in protein expression on depletion of survivin were noted as follows (marked in the proteome profiler arrays in Fig. 5A) and quantified by densitometric analysis (Fig. 5B): a marked decrease in the survivin protein level and heat shock protein 60 (hsp60) expression, a decrease in catalase and increase in HIF-1 α expression, a decrease of the pro-apoptotic factor BAD, a moderately but significantly increased expression of death receptor CD95/Fas, and a marked upregulation of TRAIL R2/DR5. No changes in the expression levels of p21^{waf/cip} and p27^{kip} were observed. It was of particular interest whether survivin RNAi led to intrinsic apoptosis via activation of effector caspase 3. As shown in Fig. 5A and in the quantitative analysis of protein expression profiles (Fig. 5B), the amounts of pro-caspase 3 and of activated caspase 3 were not affected by survivin knockdown in our experimental setting, compared with shLuc controls. To investigate whether this result could be recapitulated in other glioma cell lines, we additionally silenced survivin in H4, U343-MG, and U87-MG cells and also found no signals for cleaved pro-caspase 3 after RNAi of survivin in Western blot analyses (Fig. 5C).

Increase of Cell Death Receptor TRAIL R2 Upon Survivin Knockdown Render Glioma Cells More Susceptible to NK Cells

Because we observed a profound increase in the steady-state expression levels of the death receptor TRAIL R2/DR5 in U373-MG glioma cells upon knockdown of survivin (see Fig. 5A and B), it was of special interest whether human immune effector cells—in particular, NK cells—show enhanced lysis of these glioma cells. Therefore, human NK cells were prepared from peripheral blood, expanded, and cocultured with shRNA-treated glioma cells. The expression of CD95L and TRAIL on activated NK cells was confirmed by FACS analysis (data not shown). In line with the results of the proteome profiler assay, FACS analysis revealed that H4, U373-MG, U343-MG, and U87-MG cells transduced with shLuc displayed a surface expression of the death receptor TRAIL-R2/DR5A (Fig. 6A). Also, TRAIL-R2/DR5 expression was further increased after knockdown of survivin, as revealed by analysis of the mean fluorescence intensities of TRAIL-R2/DR5-stained cells (Fig. 6A and B). On the other hand, no significant increase in CD95/Fas levels were noted upon survivin inhibition in H4, U373-MG, U343-MG, and U87-MG cells (data not shown). ⁵¹Cr release assays demonstrated that in vitro expanded and interleukin-2 activated NK cells—in particular, at higher effector-target ratios—showed an increased basal cytotoxic reaction against shLuc-treated H4 and U373-MG glioma cells (6c). Notably, the increased surface expression of TRAIL R2/DR5 in H4 and

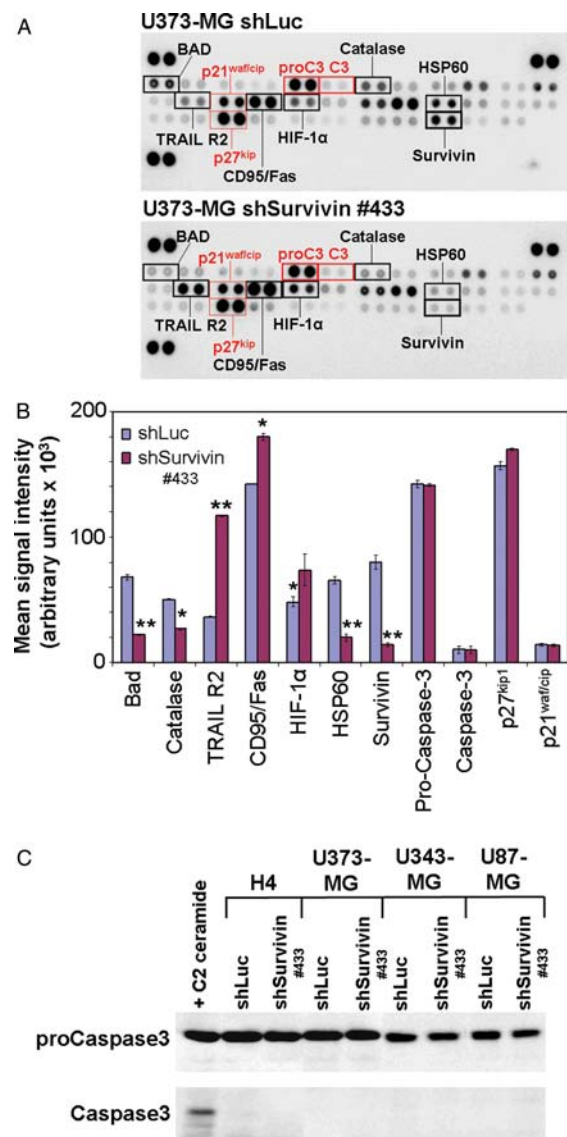


Fig. 5. Proteome profiler analysis of glioma cells upon knockdown of survivin. (A) Total protein lysates from glioma cells transduced with the shLuciferase-control vector versus cells transduced with the shSurvivin #433-vector were analyzed using an apoptosis proteome profiler blot. Depicted are representative images of the chemiluminescence signals, with differences in signal intensities between both blots showing changes in protein expression levels upon knockdown of survivin versus shLuciferase-treatment. Indicated in black boxes are significant changes in the expression levels of distinct proteins. Red boxes indicate selected proteins of interest showing no changes in protein expression levels after survivin knockdown. (B) Densitometric analysis of the proteome profiler blots depicting those proteins with significant changes in mean expression levels. Also shown are the unchanged mean expression levels of proteins involved in cell cycle arrest and caspase 3 status. (C) Western blot analysis of glioma cell lines transduced with shLuciferase (shLuc) and shSurvivin #433 (shSurv) revealed no signals indicating activated caspase 3. The levels of pro-caspase 3 remained unchanged. As positive control, H4 cells treated with 50 μ m of C2 ceramide are included. * $P < .05$. ** $P > .01$.

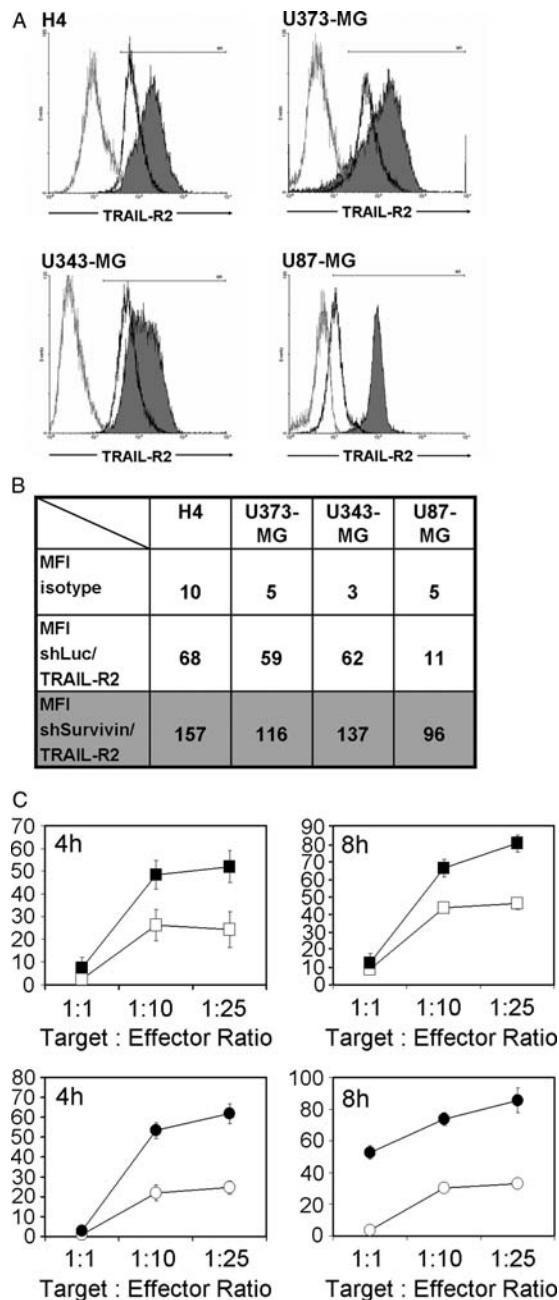


Fig. 6. NK cell cytotoxicity towards glioma cells upon survivin knockdown. (A) Knockdown of survivin increases the expression of the death receptor TRAIL R2/DR5: H4, U373-MG, U343-MG, and U87-MG glioma cells were transduced with a pRVH1-puro-vector encoding the indicated shRNAs. After 5 days, cells were stained with anti-TRAIL-R2/DR5 antibodies and measured by FACS (gray line, isotype control; black line, sh-Luc-transduced cells stained for TRAIL-R2/DR5; gray histogram, sh-Survivin #433-transduced cells stained for TRAIL-R2/DR5). (B) Quantification of TRAIL R2/DR5 expression levels by calculating the mean fluorescence intensities (MFIs) measured in FACS. Note the depicted increase in TRAIL R2/DR5 signal intensities in the glioma cells with knockdown of survivin. (C) Allogeneic human NK cells show increased cytotoxicity towards glioma cells with reduced survivin expression. NK cells were incubated with 51 chromium-loaded H4 and U373-MG

U373-MG cells transduced with shSurvivin further significantly enhanced glioma cell lysis after incubation with NK cells (Fig. 6C).

Therapeutic Knockdown of Survivin Attenuates Growth of Established Subcutaneous Glioma Xenografts and Improves Survival of Mice in an Orthotopic Glioma Model

In a next step, we sought to set up an experimental therapy approach using exogenously delivered siRNA molecules targeting survivin. We employed a low-molecular weight polyethylenimine (PEI F25-LMW) to complex and deliver siRNA targeting survivin (siSurvivin) in NMRI^{nu/nu} mice bearing established subcutaneous U373-MG tumors. The PEI/siRNA complexes were given systemically by intraperitoneal injections starting at day 1 (Fig. 7A). As negative controls, we included groups of tumor-bearing mice treated with a PEI-complexed control siRNA targeting firefly luciferase (siLuc) or, to exclude nonspecific effects of the PEI carrier on tumor growth, treated with PBS. Although the tumors of the control mice and of the siLuc-treated mice grew substantially and with similar growth rates, tumor growth in siSurvivin-treated mice was markedly attenuated. Differences in tumor sizes between specific treatment and control groups reached statistical significance at day 11 after start of PEI/siRNA treatment (Fig. 7A). In line with this observation, the mean tumor masses of excised siSurvivin-treated tumors upon termination of the experiment at day 21 after treatment start were lower, compared with the mean tumor mass of the PBS- or siLuc-treated control mice (data not shown). To determine intra-tumoral survivin expression levels, QPCR analysis using specific primers for human survivin and actin was performed. Due to the small sizes of the siSurvivin-treated tumors, only 3 tumors could be analyzed in this group, and they were compared with results for 7 siLuc-treated tumors and 7 control tumors. Remaining tumors samples were used for histological analysis. The analysis of survivin mRNA revealed a >3-fold lower expression in siSurvivin-treated tumors, compared with siLuc-treated or -untreated (PBS) control tumors (Fig. 7B). The histological analysis of siSurvivin-treated U373-MG tumors revealed frequently tumor cells with enlarged nuclei and tumor cells with multiple nuclei, whereas no such gross morphological changes were evident in the siLuc-treated controls (Fig. 7C; asterisk and arrowheads, respectively). In addition, atypical metaphase figures (propeller-like alignment of chromosomes) were detected in tumor

glioma cells at different effector to target ratios. H4 glioma cells were transduced with shLuc (open squares) or shSurvivin #433 (black squares). In parallel experiments, U373-MG glioma cells transduced with shLuc (open circles) or shSurvivin #433 (black circles) were probed against NK cells. The cytotoxic response of NK cells was measured after 4 h and 8 h.

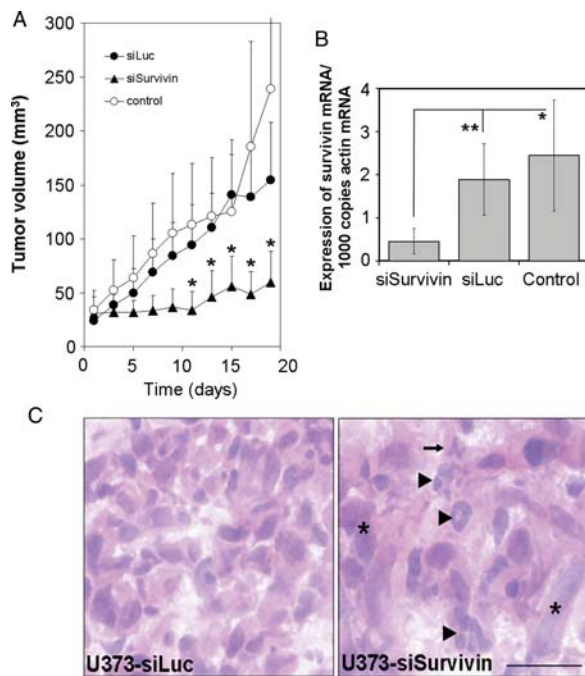


Fig. 7. Anti-tumor effects in established tumor xenografts upon therapeutic knockdown of survivin through polyethylenimine (PEI)-complexed siRNA. (A) U373-MG glioma cells were subcutaneously transplanted in the right flank of NMRI^{nu/nu} mice. After establishment of tumors, mice were randomized and treated every second day by intraperitoneal injection of (i) PEI-complexed, survivin-specific siRNA (siSurv; $n = 11$) or, as negative controls, (ii) PEI-complexed unrelated siRNA (firefly luciferase, siLuc; $n = 11$) or (iii) PBS ($n = 10$). The mean \pm standard error of the mean (SEM) of tumor volumes is shown at the indicated time points after treatment start. The treatment with PEI-complexed siSurvivin significantly attenuates tumor growth, with statistical significance ($*P < .05$) being reached 10 days after treatment start at day 1. (B) Quantitative real-time polymerase chain reaction analysis of survivin expression levels in tumors of control mice ($n = 7$) and of mice treated with PEI-complexed siSurv ($n = 3$) and siLuc ($n = 7$). The mean \pm SEM of survivin transcript levels is shown. $*P < .05$. $**P < .01$. (C) Hematoxylin-eosin staining of tumor cryosections reveal multinuclear cells (arrowheads) and huge nuclei (asterisks) in siSurvivin-treated tumors. Also note the atypical propeller-like mitotic figure (arrow) in the siSurvivin-treated tumor.

xenografts upon survivin knockdown (Fig. 7C, arrow). No signs of infiltrating leukocytes were observed in any analyzed tumor sample.

To exclude the possibility that an unspecific response of the innate immune system accounts for the observed anti-tumoral effects, NMRI^{nu/nu} and C57BL/6 mice were treated with PEI-complexed siLuc or siSurvivin, respectively, and levels of serum IFN- α were measured. In all mice, the levels of IFN- α were less than the limit of detection, whereas in polyinosinic-polycytidylic acid-treated C57BL/6-positive control mice, a mean (\pm SD) IFN- α level of 18 ± 0.5 pg/mL was found (data not shown).

For a more relevant in vivo validation we tested whether treatment of orthotopic U87-MG xenografts with PEI-complexed siRNA targeting survivin results in a better survival of NMRI^{nu/nu} mice. Three days after transplantation of the glioma cells, mice were treated for 10 days with daily stereotactical injections of PEI-complexed siRNAs targeting survivin or luciferase. No toxic side effects of PEI/siRNA complexes were observed. Analysis at day 17 after tumor cell transplantation revealed smaller tumors in mice treated with PEI/siSurvivin, compared with the control group treated with PEI/siLuc (Fig. 8A). Concomitantly, indirect immunofluorescence analysis of survivin expression showed decreased immunoreactivity in PEI/siSurvivin-treated tumors versus the PEI/siLuc controls (Fig. 8B). The analysis of the survival of the mice (ie, the time period before the onset of neurological symptoms) revealed a significant improvement of the mean survival time for PEI/siSurvivin-treated tumor-bearing mice (23 days) compared with the PEI/siLuc-treated negative controls (18 days; Fig. 8C). Additional immunohistochemical analysis of the tumors showed that siSurvivin treatment induced a 2-fold reduction in the percentage of Ki67-positive cells, indicating loss of proliferation capacity (Fig. 8D). The possibility that the observed effects were due to increased apoptosis in the siSurvivin-treated tumors was rendered unlikely because a TUNEL assay revealed an only slight and statistically insignificant increase in apoptosis in siSurvivin-treated tumors (mean apoptosis index \pm SD, $0.21\% \pm 0.04\%$) compared with siLuc-treated tumors (mean apoptosis index \pm SD, $0.11\% \pm 0.09\%$) (Fig. 8E).

Discussion

GBM, classified as glioma World Health Organization grade IV, is the most frequent and malignant brain tumor which is mostly resistant to conventional therapies.¹⁻³ Consequently, novel therapeutic options for the treatment of malignant gliomas are warranted. siRNA is evolving as a promising strategy for cancer therapy due to its high efficiency and specificity in blocking target mRNA expression.^{6,34,35} For treating experimental gliomas, we chose survivin as target because it is strongly expressed in tumors and barely detected in normal differentiated tissues.⁸ Survivin expression has also been reported in human gliomas,⁹ and expression of survivin is found in glioma- and glioblastoma-derived cell lines.²⁶ Furthermore, the knockdown of survivin cannot be fully compensated by the upregulation of other members of the inhibitor of apoptosis family because, beside its role in anti-apoptosis, survivin plays a unique and pivotal role in the spindle checkpoint and cytokinesis.^{25,29}

Here, we report efficient knockdown of survivin expression in glioma cell lines and primary glioma cell lines using retrovirus-delivered shRNAs targeting survivin. Glioma cells with loss of survivin developed mitotic defects resulting in polyploidy, and we showed decreased

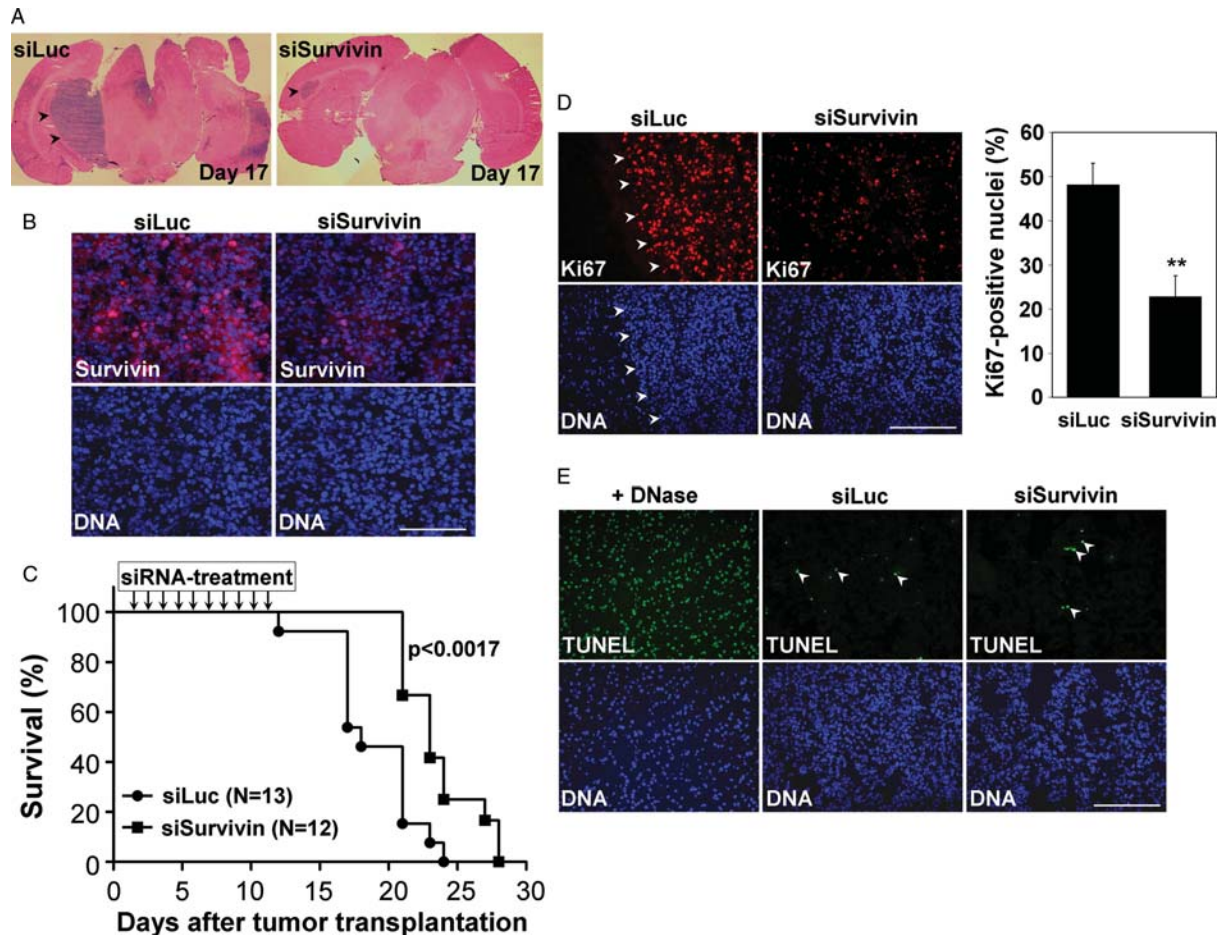


Fig. 8. Intracranially administered polyethylenimine (PEI)-complexed siRNA targeting survivin attenuates cellular proliferation and improves survival of mice in an orthotopic glioma model. (A) Images showing hematoxylin-eosin-stained slices of U87-MG intracranial tumors 17 days after tumor cell transplantation. Tumors are indicated by arrowheads. Note the prominent U87-MG tumor in the siLuc treated mouse and the smaller tumor size in siSurvivin-treated mouse. (B) Indirect immunofluorescence analysis using anti-survivin antibody showing decreased survivin immunosignals in siSurvivin-treated tumors. (C) Kaplan-Meier-plot showing the time schedule of PEI/siRNA injections and the survival curves of the animals in the different treatment groups. Mice treated with PEI/siSurvivin showed significantly increased survival times when compared to the PEI/siLuc-treated controls. (D) Indirect immunofluorescence analysis of the proliferation marker Ki67 reveals attenuated cell proliferation in siSurvivin-treated U87-MG cells when compared to siLuc controls (** $P < .01$). Arrowheads depict the borderline between U87-MG tumor and mouse brain parenchyma. (E) Investigation of apoptosis using TUNEL assay. Arrowheads depict apoptotic cells. No significant increased apoptosis was detected in tumors treated with siSurvivin. A DNase-treated slice is included as positive control. DNA counterstaining in all fluorescence images were accomplished with Hoechst 33342. Bars in panel B represent 300 μm ; bars in panels D and E represent 200 μm .

proliferation and impaired clonogenic survival in long-term cell culture assays. In vitro analyses of the hypodiploid cell fraction in U373-MG and H4 glioma cells and primary glioma cells revealed, in most cases, increases in the fraction of apoptotic cells. However, proteome profiler arrays of survivin-shRNA-transduced U373-MG cells, and additional Western blot analysis of U373-MG, U343-MG, U87-MG, and H4 cells after survivin knockdown showed no activation of the executioner caspase 3, indicating a caspase-independent cell death mechanism. This observation is in line with findings from other reports that describe a caspase-independent induction of cell death upon silencing of survivin or upon ectopic expression of dominant-negative survivin mutants.^{16,26,36} However, some reports—in particular, those that used U251-MG

glioma cells—also have described a caspase-dependent cell death upon RNAi of survivin.^{37–39} Thus far, it is tempting to speculate whether the observed differences are cell type specific or are due to technical differences.

Survivin knockdown also resulted in a marked decrease of hsp60. Interestingly, this chaperone molecule has been reported to directly interact with survivin,⁴⁰ and RNAi-mediated reduction of hsp60 has been reported to decrease survivin expression, in particular mitochondrial survivin levels.⁴⁰ Our data suggests that, vice versa, hsp60 levels are dependent on to survivin expression. Therefore, additional studies are warranted to elucidate this survivin/HSP60 interplay. Moreover, we noted a decrease in catalase expression and increase in expression of HIF-1 α in survivin-knockdown cells. These changes in protein

expression levels were accompanied by the development of huge multinuclear cells, and we suggest that this finding might reflect some adaptation of the cells to altered intracellular reactive oxygen species and oxygen levels.

Interestingly, we found no increase in the levels of p21^{waf/cip} and p27^{kip} after RNAi of survivin in a proteome profiler array, indicating that the U373-MG glioma cells did not activate cell-cycle checkpoints. In addition, no cell-cycle arrest was detected when analyzing the DNA content of H4 cells and of 3 primary glioblastoma cell lines. In line with this, BrdU incorporation assays revealed that U373-MG and H4 cells, even with DNA contents of $\geq 4N$, still entered S-phase. We assume that a compromised checkpoint function allows ongoing DNA replications without the separation of daughter cells due to defects in cytokinesis.²⁴ The higher DNA contents in turn might result in prolonged cell cycle phases, which could explain the general decrease in the fraction of BrdU-positive cells observed in our experiments (see Fig. 2).

The knockdown of survivin led to a downregulation of the pro-apoptotic Bad molecule, whereas higher expression of the death receptor CD95/Fas and an even more pronounced increase in the steady-state expression level of the death receptor TRAIL R2/DR5 was observed. The induction of TRAIL R2/DR5 after RNAi-mediated targeting of survivin was verified using FACS-based analysis of H4, U343-MG, U373-MG, and U87-MG glioma cells. Interestingly, the increased expression of TRAIL R2/DR5 rendered H4 and U373-MG cells more susceptible to NK cells, as shown in a cytotoxic assay.

Several groups have demonstrated strong anti-cancer effects in vivo upon RNAi-mediated survivin knockdown. However, because of problems in pharmacokinetics and cellular uptake of RNAi effector molecules, siRNAs/shRNAs or shRNA-encoding vectors, most studies were based on tumor cells transfected with siRNAs or shRNA-encoding vectors ex vivo prior to transplantation and in vivo analysis. Using this approach, anti-tumoral effects were shown in xenografts established from in vitro-transfected esophageal squamous carcinoma,⁴¹ gastric cancer,⁴² pancreatic cancer,⁴³ breast cancer,⁴⁴ cervical carcinoma,⁴⁴ and glioma cells.³⁸ On the other hand, only a few studies on the RNAi-mediated knockdown of survivin in already established tumors have been reported. One simple treatment approach made use of direct intratumoral injection of a shRNA-expression vector targeting survivin mRNA. In this study, a reduction of xenografted rhabdomyosarcoma tumor growth was observed.⁴⁵ More recently George et al.³⁹ reported attenuated growth of orthotopic U251-MG gliomas when stereotactically transfected with an DNA plasmid encoding a shRNA targeting survivin. Other reports have described antitumor effects in xenografted hepatocellular carcinoma, colorectal carcinoma, and non-small cell lung carcinoma upon the delivery of shRNA-encoding constructs against survivin using adenoviral vectors and replication defective lentiviral

vectors.^{46–48} Likewise, an anti-cancer effect on subcutaneous U251-MG glioma xenografts upon direct intratumoral injection of adenoviral vectors encoding a survivin-specific shRNA has been reported.³⁷

However, because the in vivo delivery of shRNA-encoding plasmids is mostly ineffective, and because application of viral shRNA delivery systems in patients is generally hampered due to safety concerns and limited routes of application, we performed a therapeutic knockdown of survivin using a nonviral, polymer-based carrier system for systemic siRNA delivery.

Previously, certain PEIs have been established as reagents for complexation and cellular delivery of siRNA in vitro and in vivo.^{49–51} This siRNA delivery platform allowed the systemic application of unmodified siSurvivin siRNA molecules at a dose of 400 $\mu\text{g}/\text{kg}$ body weight for an experimental therapy of subcutaneous glioma xenografts. More specifically, we demonstrate that treatment of established U373-MG subcutaneous xenografts using PEI-complexed siRNA targeting survivin led to a decrease of survivin mRNA levels in tumors and resulted in markedly attenuated tumor growth. The analysis of serum samples obtained from PEI/siRNA-treated immunodeficient NMRI^{nu/nu}, as well as immune-competent C57BL/6 mice, did not reveal any IFN response, indicating that the PEI/siRNA treatment of mice did not activate the innate immune system. Notably, the histological investigation of the siSurvivin-treated tumors revealed an increase in the appearance cells bearing large nuclei, as well as increased numbers of cells having multiple nuclei, both being frequently observed phenotypes caused by interference with survivin function.^{24,28,45,52} In connection with our QPCR data demonstrating decreased survivin expression levels in the siSurvivin-treated glioma xenografts, we demonstrate that the intraperitoneally injected PEI/siRNA complexes are able to reach the subcutaneous glioma xenografts, as shown elsewhere,⁵⁰ and that PEI/siRNA-mediated survivin knockdown exerts profound antitumor effects.

We further extended our studies toward more aggressively proliferating U87-MG cells in an orthotopic glioma model. Because the brain is an “immune privileged” organ lacking the components of the lymphatic system, a systemic delivery of siRNA to the tumor can be envisioned only via the bloodstream. However, probably because of the blood-brain barrier, previous studies on the biodistribution of PEI F25-LMW/siRNA after intraperitoneal injection revealed only very little siRNA uptake into the brain. The same study showed that intravenous injection of PEI/siRNA-complexes via the tail vein resulted in siRNA accumulation, mostly in the liver and lungs.³² These findings are in line with results from other groups demonstrating that the transport of nanoparticles across the blood-brain barrier will strongly rely on ligand-mediated, “targeted” delivery strategies or “Trojan horse” concepts (for review see Schulze et al.⁵³). Despite the possibility of a somewhat leakier blood-brain barrier, this may also apply to glioblastomas. Therefore, we performed a local PEI/siRNA-treatment of orthotopic U87-MG gliomas that

circumvents the blood-brain barrier. The clinical relevance of this approach is supported by many clinical studies that focused on glioma treatment and used local delivery methods of compounds such as paclitaxel, IL13-PE38QQR, or TGF- β 2 antisense.^{54–56} In the long run, however, we and others aim to develop of ligand-functionalized nanoparticles for the targeted delivery of nucleic acids, allowing systemic administration and leading to higher efficacy. In summary, by applying consecutive stereotactical injections of PEI-complexed siRNA targeting survivin at the tumor site, we significantly improved the survival time of mice. Additional analysis of the proliferation marker Ki67 revealed that siSurvivin-treated intracranial U87-MG tumors had a decreased proliferation capacity, whereas induction of apoptosis was barely visible.

In conclusion, our results show—to our knowledge, for the first time—that the knockdown of survivin expression by exogenous, nonviral delivery of PEI-complexed siRNA molecules significantly inhibits the growth of established gliomas *in vivo*. Our *in vitro* and *in vivo* data indicate that loss of survivin leads to defective mitosis and increased endoreplication in tumor cells, finally leading to decreased proliferation and mitotic catastrophe. Notably, glioma cells with survivin knockdown also displayed significantly more TRAIL R2/DR5 on the cell surface, which increased the cytotoxic responses of human NK cells *in vitro*. However, because we used immunodeficient NMRI^{nu/nu} mice as host for the xenografts, an appropriate immune response *in vivo* appears unlikely in our experiments; in line with this assumption, the histological analysis of glioma xenografts revealed no infiltration of leukocytes (ie, NK cells present in immunodeficient NMRI^{nu/nu}) into the treated tumors. This indicates that the antitumor effects of PEI/siSurvivin treatment observed here are only based on “direct” intracellular effects of survivin knockdown. In contrast, an experimental PEI/siSurvivin therapy approach targeting transplanted syngeneic glioma cells in

immunocompetent mice will address the question whether the host immune system can even further promote anti-glioma effects caused by the knockdown of survivin. However, for the development of a systemic PEI/siRNA-therapy of gliomas, additional improvements of PEI-siRNA carrier molecules are warranted. Modifications might include covalent coupling of maltose- or polyethylenglycol molecules for minimizing unspecific uptake and additional conjugation of antibodies (ie, transferrin receptor antibody) and ligands (ie, transferrin, lactoferrin), which hold promise for a receptor-mediated transcytosis in brain endothelial cells.^{57–59}

In the view of the efficiency and specificity of RNA interference in connection with the development of advanced carrier systems, siRNA therapies for the knockdown of target genes, such as survivin, may be useful in therapy of gliomas and other cancers.

Acknowledgments

We thank F. Zachow and B. Goldberg for excellent technical assistance. pMD.G2 was kindly provided by D. Trono (University of Geneva, Switzerland). The pRVH-1 and pRVH1-puro vectors were kindly provided by S. Schuck and K. Simons (MPI for Cell Biology and Genetics, Dresden, Germany).

Conflict of interest statement. None declared.

Funding

Wilhelm Sander Stiftung (2008.065.1 to A.T.), Deutsche Krebshilfe (106992 to A.A.), Deutsche Forschungsgemeinschaft (Forschergruppe 627 ‘Nanohale’, AI 24/6-1 to A.A.).

References

1. Surawicz TS, Davis F, Freels S, Laws ER, Jr, Menck HR. Brain tumor survival: results from the National Cancer Data Base. *J Neurooncol.* 1998;40(2):151–160.
2. Davis FG, Kupelian V, Freels S, McCarthy B, Surawicz T. Prevalence estimates for primary brain tumors in the United States by behavior and major histology groups. *Neuro Oncol.* 2001;3(3):152–158.
3. Grossman SA, Batarra JF. Current management of glioblastoma multiforme. *Semin Oncol.* 2004;31(5):635–644.
4. Hou LC, Veeravagu A, Hsu AR, Tse VC. Recurrent glioblastoma multiforme: a review of natural history and management options. *Neurosurg Focus.* 2006;20(4):E5.
5. Quick A, Patel D, Hadziahmetovic M, Chakravarti A, Mehta M. Current therapeutic paradigms in glioblastoma. *Rev Recent Clin Trials.* 2010;5(1):14–27.
6. Ashihara E, Kawata E, Maekawa T. Future prospect of RNA interference for cancer therapies. *Curr Drug Targets.* 2010;11(3):345–360.
7. Ambrosini G, Adida C, Altieri DC. A novel anti-apoptosis gene, survivin, expressed in cancer and lymphoma. *Nat Med.* 1997;3(8):917–921.
8. Velculescu VE, Madden SL, Zhang L, et al. Analysis of human transcriptomes. *Nat Genet.* 1999;23(4):387–388.
9. Das A, Tan WL, Teo J, Smith DR. Expression of survivin in primary glioblastomas. *J Cancer Res Clin Oncol.* 2002;128(6):302–306.
10. Chakravarti A, Noll E, Black PM, et al. Quantitatively determined survivin expression levels are of prognostic value in human gliomas. *J Clin Oncol.* 2002;20(4):1063–1068.
11. Kajiwara Y, Yamasaki F, Hama S, et al. Expression of survivin in astrocytic tumors: correlation with malignant grade and prognosis. *Cancer.* 2003;97(4):1077–1083.
12. Saito T, Arifin MT, Hama S, et al. Survivin subcellular localization in high-grade astrocytomas: simultaneous expression in both nucleus and cytoplasm is negative prognostic marker. *J Neurooncol.* 2007;82(2):193–198.

13. O'Connor DS, Schechner JS, Adida C, et al. Control of apoptosis during angiogenesis by survivin expression in endothelial cells. *Am J Pathol*. 2000;156(2):393–398.
14. Shin S, Sung BJ, Cho YS, et al. An anti-apoptotic protein human survivin is a direct inhibitor of caspase-3 and -7. *Biochemistry*. 2001;40(4):1117–1123.
15. Song Z, Yao X, Wu M. Direct interaction between survivin and Smac/DIABLO is essential for the anti-apoptotic activity of survivin during taxol-induced apoptosis. *J Biol Chem*. 2003;278(25):23130–23140.
16. Liu T, Brouha B, Grossman D. Rapid induction of mitochondrial events and caspase-independent apoptosis in survivin-targeted melanoma cells. *Oncogene*. 2004;23(1):39–48.
17. Li F, Ambrosini G, Chu EY, et al. Control of apoptosis and mitotic spindle checkpoint by survivin. *Nature*. 1998;396(6711):580–584.
18. Mirza A, McGuirk M, Hockenberry TN, et al. Human survivin is negatively regulated by wild-type p53 and participates in p53-dependent apoptotic pathway. *Oncogene*. 2002;21(17):2613–2622.
19. Hoffman WH, Biade S, Zilfou JT, Chen J, Murphy M. Transcriptional repression of the anti-apoptotic survivin gene by wild type p53. *J Biol Chem*. 2002;277(5):3247–3257.
20. Pennati M, Folini M, Zaffaroni N. Targeting survivin in cancer therapy. *Expert Opin Ther Targets*. 2008;12(4):463–476.
21. Fraser AG, James C, Evan GI, Hengartner MO. Caenorhabditis elegans inhibitor of apoptosis protein (IAP) homologue BIR-1 plays a conserved role in cytokinesis. *Curr Biol*. 1999;9(6):292–301.
22. Speliotes EK, Uren A, Vaux D, Horvitz HR. The survivin-like C. elegans BIR-1 protein acts with the Aurora-like kinase AIR-2 to affect chromosomes and the spindle midzone. *Mol Cell*. 2000;6(2):211–223.
23. Uren AG, Wong L, Pakusch M, et al. Survivin and the inner centromere protein INCENP show similar cell-cycle localization and gene knockout phenotype. *Curr Biol*. 2000;10(21):1319–1328.
24. Temme A, Rieger M, Reber F, et al. Localization, dynamics, and function of survivin revealed by expression of functional survivinDsRed fusion proteins in the living cell. *Mol Biol Cell*. 2003;14(1):78–92.
25. Wheatley SP, Carvalho A, Vagnarelli P, Earnshaw WC. INCENP is required for proper targeting of survivin to the centromeres and the anaphase spindle during mitosis. *Curr Biol*. 2001;11(11):886–890.
26. Temme A, Herzig E, Weigle B, et al. Inhibition of malignant glioma cell growth by a survivin mutant retrovirus. *Hum Gene Ther*. 2005;16(2):209–222.
27. Li F, Ackermann EJ, Bennett CF, et al. Pleiotropic cell-division defects and apoptosis induced by interference with survivin function. *Nat Cell Biol*. 1999;1(8):461–466.
28. Lens SM, Wolthuis RM, Klompaker R, et al. Survivin is required for a sustained spindle checkpoint arrest in response to lack of tension. *EMBO J*. 2003;22(12):2934–2947.
29. Honda R, Korner R, Nigg EA. Exploring the functional interactions between Aurora B, INCENP, and survivin in mitosis. *Mol Biol Cell*. 2003;14(8):3325–3341.
30. Elbashir SM, Harborth J, Weber K, Tuschl T. Analysis of gene function in somatic mammalian cells using small interfering RNAs. *Methods*. 2002;26(2):199–213.
31. Soneoka Y, Cannon PM, Ramsdale EE, et al. A transient three-plasmid expression system for the production of high titer retroviral vectors. *Nucleic Acids Res*. 1995;23(4):628–633.
32. Hobel S, Koburger I, John M, et al. Polyethylenimine/small interfering RNA-mediated knockdown of vascular endothelial growth factor in vivo exerts anti-tumor effects synergistically with bevacizumab. *J Gene Med*. 2010;12(3):287–300.
33. Brockmann MA, Westphal M, Lamszus K. Improved method for the intracerebral engraftment of tumour cells and intratumoural treatment using a guide screw system in mice. *Acta Neurochir (Wien)*. 2003;145(9):777–781.
34. Stevenson M. Therapeutic potential of RNA interference. *N Engl J Med*. 2004;351(17):1772–1777.
35. Shankar P, Manjunath N, Lieberman J. The prospect of silencing disease using RNA interference. *JAMA*. 2005;293(11):1367–1373.
36. Croci DO, Cogno IS, Vittar NB, et al. Silencing survivin gene expression promotes apoptosis of human breast cancer cells through a caspase-independent pathway. *J Cell Biochem*. 2008;105(2):381–390.
37. Uchida H, Tanaka T, Sasaki K, et al. Adenovirus-mediated transfer of siRNA against survivin induced apoptosis and attenuated tumor cell growth in vitro and in vivo. *Mol Ther*. 2004;10(1):162–171.
38. Zhen HN, Li LW, Zhang W, et al. Short hairpin RNA targeting survivin inhibits growth and angiogenesis of glioma U251 cells. *Int J Oncol*. 2007;31(5):1111–1117.
39. George J, Banik NL, Ray SK. Survivin knockdown and concurrent 4-HPR treatment controlled human glioblastoma in vitro and in vivo. *Neuro Oncol*. 2010;12(11):1088–1101.
40. Ghosh JC, Dohi T, Kang BH, Altieri DC. Hsp60 regulation of tumor cell apoptosis. *J Biol Chem*. 2008;283(8):5188–5194.
41. Wang Y, Zhu H, Quan L, et al. Downregulation of survivin by RNAi inhibits the growth of esophageal carcinoma cells. *Cancer Biol Ther*. 2005;4(9):974–978.
42. Chen T, Deng C. Inhibitory effect of siRNA targeting survivin in gastric cancer MGC-803 cells. *Int Immunopharmacol*. 2008;8(7):1006–1011.
43. Shen YM, Yang XC, Song ML, Qin CH, Yang C, Sun YH. Growth inhibition induced by short hairpin RNA to silence survivin gene in human pancreatic cancer cells. *Hepatobiliary Pancreat Dis Int*. 2010;9(1):69–77.
44. Li QX, Zhao J, Liu JY, et al. Survivin stable knockdown by siRNA inhibits tumor cell growth and angiogenesis in breast and cervical cancers. *Cancer Biol Ther*. 2006;5(7):860–866.
45. Caldas H, Holloway MP, Hall BM, Qualman SJ, Altura RA. Survivin-directed RNA interference cocktail is a potent suppressor of tumour growth in vivo. *J Med Genet*. 2006;43(2):119–128.
46. Zhang R, Ma L, Zheng M, et al. Survivin knockdown by short hairpin RNA abrogates the growth of human hepatocellular carcinoma xenografts in nude mice. *Cancer Gene Ther*. 2010;17(4):275–288.
47. Shen W, Wang CY, Wang XH, Fu ZX. Oncolytic adenovirus mediated Survivin knockdown by RNA interference suppresses human colorectal carcinoma growth in vitro and in vivo. *J Exp Clin Cancer Res*. 2009;28:81.
48. Liu GF, Zhao QG, Si L, Cao YG, Li GY, Wang LX. Effects of survivin interference RNA on non-small cell lung carcinoma. *Clin Invest Med*. 2009;32(6):E225.
49. Urban-Klein B, Werth S, Abuharbeid S, Czubayko F, Aigner A. RNAi-mediated gene-targeting through systemic application of polyethylenimine (PEI)-complexed siRNA in vivo. *Gene Ther*. 2005;12(5):461–466.
50. Grzelinski M, Urban-Klein B, Martens T, et al. RNA interference-mediated gene silencing of pleiotrophin through polyethylenimine-complexed small interfering RNAs in vivo exerts antitumoral effects in glioblastoma xenografts. *Hum Gene Ther*. 2006;17(7):751–766.
51. Aigner A. Delivery systems for the direct application of siRNAs to induce RNA interference (RNAi) in vivo. *J Biomed Biotechnol*. 2006;2006(4):71659.

52. Kappler M, Bache M, Bartel F, et al. Knockdown of survivin expression by small interfering RNA reduces the clonogenic survival of human sarcoma cell lines independently of p53. *Cancer Gene Ther.* 2004;11(3):186–193.
53. Schulze D, Aigner A. Nanosystems for delivery of RNAi. In: Erdmann, VA, Reifenberger, G, Barciszewski, J, eds. *Therapeutic Ribonucleic Acids in Brain Tumors*. Springer; 2009.
54. Hau P, Jachimczak P, Schlingensiepen R, et al. Inhibition of TGF-beta2 with AP 12009 in recurrent malignant gliomas: from preclinical to phase I/II studies. *Oligonucleotides.* 2007;17(2): 201–212.
55. Lidar Z, Mardor Y, Jonas T, et al. Convection-enhanced delivery of paclitaxel for the treatment of recurrent malignant glioma: a phase I/II clinical study. *J Neurosurg.* 2004;100(3):472–479.
56. Vogelbaum MA, Sampson JH, Kunwar S, et al. Convection-enhanced delivery of cintredekin besudotox (interleukin-13-PE38QQR) followed by radiation therapy with and without temozolomide in newly diagnosed malignant gliomas: phase 1 study of final safety results. *Neurosurgery.* 2007;61(5):1031–1037.
57. Pardridge WM, Buciak JL, Friden PM. Selective transport of an anti-transferrin receptor antibody through the blood-brain barrier in vivo. *J Pharmacol Exp Ther.* 1991;259(1):66–70.
58. Pang Z, Feng L, Hua R, et al. Lactoferrin-conjugated biodegradable polymersome holding doxorubicin and tetrandrine for chemotherapy of glioma rats. *Mol Pharm.* 2010;7(6):1995–2005.
59. Laske DW, Youle RJ, Oldfield EH. Tumor regression with regional distribution of the targeted toxin TF-CRM107 in patients with malignant brain tumors. *Nat Med.* 1997;3(12):1362–1368.